Available online at www.eccomasproceedia.org
Eccomas Proceedia COMPDYN (2025) 805- 815

ECCOMAS
Proceedia

COMPDYN 2025
10th ECCOMAS Thematic Conference on
Computational Methods in Structural Dynamics and Earthquake Engineering
M. Papadrakakis, M. Fragiadakis (eds.)
Rhodes Island, Greece, 15-18 June 2025

RESPONSE OF EARTHQUAKE-DAMAGED REINFORCED CONCRETE COLUMNS UNDER NATURAL FIRE EXPOSURE: A NUMERICAL STUDY

Anand Kumar[1] and P. Ravi Prakash[1,2]

[1]Department of Civil and Infrastructure Engineering
Indian Institute of Technology Jodhpur, Rajasthan, India, 342030.
e-mail: kumar.263@iitj.ac.in

[2] School of Artificial Intelligence and Data Science
Indian Institute of Technology Jodhpur, Rajasthan, India, 342030.
e-mail: rp@iitj.ac.in

Abstract. *Reinforced concrete (RC) columns serve as primary load-bearing elements in building structures. These are susceptible to significant damage due to accidental hazards such as earthquakes and fires, during service life. Large earthquakes may even trigger simultaneous fire outbreaks. However, the current building standards do not consider the possibility of post earthquake fire (PEF) scenarios in design. This study develops a numerical framework in GID-OpenSees to analyze RC columns under fire, with a focus on PEF scenarios. The framework employs an Euler-Bernoulli based beam-column finite element with fiber-discretized section for thermomechanical analysis. A separate 2D finite element analysis is performed over the section to determine the temperature field within the element due to fire. A one-way coupling of the temperature field and the mechanical field is achieved through the fibers. Newly developed uniaxial material models for concrete and reinforcement are implemented to ensure accurate analysis. Few validation studies are presented against the experimental results to showcase the efficacy of the framework. Subsequently, two sets of RC column—one with prior earthquake damage and another without damage—are analyzed under natural fire exposure. Sections damaged due to earthquake (spalled sections) are modelled by removing the affected fibers from the sections. A parametric study are presented using the validated model, by varying the earthquake damage level, axial load level, and the fire-exposed sides of the column. The response of the column in terms of displacement histories and fire resistance times are shown and compared with the undamaged column in each case. The findings of this study provide valuable insights about the fire resilience of earthquake-damaged RC columns.*

Keywords: Reinforced Concrete Columns, Fire Resistance, Fire Following Earthquake, OpenSees.

ISSN:2623-3347 © 2025 The Authors. Published by Eccomas Proceedia.
Peer-review under responsibility of the organizing committee of COMPDYN 2025.
doi: 10.7712/120125.12692.25114

1 INTRODUCTION

Reinforced concrete (RC) columns are essential load-bearing elements in building structures. Extreme hazards such as earthquakes and fires can severely compromise the structural integrity of RC columns throughout their service life. One particular concern is the post-earthquake fire (PEF) scenario, where earthquake damage increases the vulnerability of RC elements to subsequent fires. Historical events, like the 1906 San Francisco earthquake and the 1995 Kobe earthquake in Japan, have demonstrated the devastating effects of PEF. In such events, seismic activity can cause structural damage that creates pathways for fire to spread in multiple neighborhoods. The combined effects of seismic damage and subsequent conflagration intensify the destruction [1]. Despite these risks, modern building codes and design standards often address earthquakes and fires as separate hazards, with little consideration for multi-hazard scenarios including PEF.

Current building codes such as NRCC 2005 [2], EN 1992-1-2 [3], and ACI 216.1-14 [4] provide typical fire-resistance rating requirements for specific building elements. However, these provisions are developed for normal fire exposure condition and do not consider the impact of prior seismic damage. The performance-based design approach necessitates that the effect of seismic damage on the fire resistance behavior of the structural element be determined, even without subsequent fire development [1].

Besides code-based provisions, the fire resistance of reinforced concrete columns is commonly assessed through experimental investigations and numerical simulations. While substantial research exists for conventional fire scenarios (without earthquake) [5] , studies on PEF scenarios remain limited [6]. Evaluating fire resistance under PEF scenarios is more complex due to multiple influencing factors. A primary challenge lies in quantifying structural damage after seismic events, where impacts may range from minor to severe depending on earthquake magnitude and structural characteristics. In RC columns, such damage manifests as both geometric alterations (cracking, spalling-induced section loss, reinforcement buckling, and permanent deformations) and mechanical deterioration (degraded material properties). Recent experimental work by Chinthapalli and Agrawal [13] examined PEF performance of RC columns using a novel testing protocol. Their methodology involved first damaging the columns to a predetermined level of cyclic earthquake loading in presence of an axial compressive load followed by heating the columns under ISO 834 fire for a 1-h duration and again subjecting them to pure axial compressive load until failure. The results demonstrated a significant reduction in fire resistance for earthquake-damaged columns compared to undamaged ones. While experimental testing provides reliable means to assess PEF behavior of RC column, such methods are often complex, time-consuming, and costly. Numerical simulations offers a more efficient alternative for analyzing the fire resistance behavior of RC columns under PEF scenarios.

Numerical assessment of PEF performance in RC elements typically follows a three-stage procedure: (1) seismic damage evaluation, which involves dynamic analysis of structure under site-specific ground motions, (2) thermal exposure modeling using either standard (e.g., ISO 834) or physics-based fire curves, and (3) thermo-mechanical analysis incorporating temperature-dependent constitutive models and geometric nonlinear effects. The above steps can be implemented through finite element based computational program. This approach has been implemented by researchers such as Behnam and Ronagh [7, 8] to investigate the PEF behavior of the RC frames. While some studies like Vitorino et al. [9, 10] used simplified approach and employed damage proxies (e.g., reduced concrete cover thickness categorized by performance states: Immediate Occupancy, Life Safety, and Collapse Prevention), rather than explicit seismic simulation. However, a significant limitation of most existing studies is their reliance on the standard ISO 834 fire curve, which represents only the heating phase of fire development. Real building fires include both heating and cooling phases. The cooling phase of fire presents a critical scenario where surface temperatures decrease while core temperatures in RC members may continue to rise, which potentially causes delayed structural failure [5]. This underscores the necessity for more comprehensive PEF performance assessments considering natural (real) fire conditions.

This study investigates the PEF performance of RC columns using a thermo-mechanical analysis framework developed in GiD-OpenSees. The analysis employs a two-level discretization scheme in OpenSees, where the structure is modeled using beam-column elements with fiber sections, while 2D conductive elements are used for thermal (heat transfer) analysis. Newly developed temperature-dependent uniaxial material models for concrete and steel are implemented to accurately capture PEF behavior of the RC columns. Few experimental validation is provided to demonstrate the efficacy of the model. The research specifically examines the fire resistance behavior of RC columns with predefined earthquake-damage under natural fire conditions. Influence of variable such as various fire scenarios, fire exposure orientations and load ratios are investigated.

2 GID-OPENSEES FRAMEWORK

The PEF analysis is performed using a simplified approach similar to those utilized by Vitorino et al. [9, 10], where earthquake damage is simulated by reducing the concrete cover at specified locations in the column section. The damaged columns then undergo thermo-mechanical analysis under combined loading and fire exposure. The analysis follows a sequential two-step procedure: (1) thermal analysis solving heat transfer equations to obtain time-dependent temperature distributions, and (2) mechanical analysis, where the temperature time history as determined from the thermal analysis is fed to the structural model to perform stress analysis. Inelastic deformation and temperature dependent material properties are used during the mechanical analysis. A brief overview of the thermo-mechanical analysis framework developed in GiD-OpenSees is presented below, with further details available in the authors' previous work [11].

2.1 Thermo-mechanical analysis

The thermo-mechanical analysis begins with thermal analysis using 2D conductive elements (HTBlock) to solve the heat conduction equation across the cross-section. The governing equation that account for 2D heat conduction within the concrete and combined convection-radiation at exposed surfaces is solved at each time step. Nonlinear solution techniques are employed to handle temperature-dependent material properties and radiative boundary conditions. For fire-exposed surfaces, the convection coefficient is set to 25 kW/m2, in line with EN 1992-1-2 [3] for standard fire exposure, while for unexposed surfaces, it is set to 4 kW/m2. The emissivity of the surface is assumed to be 0.85. The thermal properties of concrete (thermal conductivity and specific heat) are adopted in accordance with EN 1992-1-2 [3] for siliceous concrete aggregate. Due to the negligible cross-sectional area of steel compared to concrete in RC sections, the presence of steel was disregarded in the thermal analysis. The resulting temperature distribution is mapped to the corresponding fibers for the mechanical analysis.

The mechanical analysis is conducted using the Euler-Bernoulli beam finite element (*DispBeamColumn3dThermal*) with fiber discretized section (*FiberSectionGJThermal*). The *Disp-*

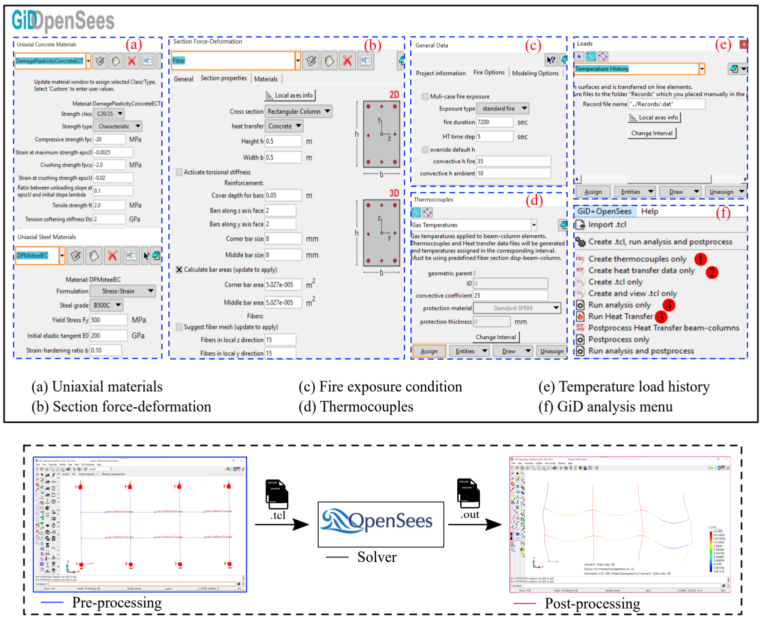

Figure 1: GiD-OpenSees simulation interface.

BeamColumn3DThermal element features six degrees of freedom (three translational and three rotational) at each node in the global coordinate system. The geometric nonlinearity effect is considered via co-rotational transformation. The cross-section of the element comprises several fibers, with each fiber assigned a temperature-dependent uniaxial stress-strain law. Such approach facilitates the consideration of nonlinear thermal gradient, temperature dependent material properties and spatial variability in inelasticity. The constitutive models are based on the strain decomposition as follows:

$$\varepsilon_{\text{tot}} = \varepsilon_{\sigma} + \varepsilon_{\text{th}} + \varepsilon_{\text{tr}}, \tag{1}$$

where ε_{tot} represents total strain which is obtained from spatial derivatives of the displacement field; ε_{σ} represents the mechanical strain which contains the elastic and plastic part of the strain; ε_{th} represents the thermal strain that dependent only on the temperature; ε_{tr} represents the transient creep in concrete. The sectional forces are computed through fiber stress integration, with equilibrium equations formulated using shape functions and solved iteratively via Newton-Raphson methods. An implicit dynamic approach with Newmark integration is implemented to address numerical convergence issue due to high-temperature softening instabilities.

The thermo-mechanical analysis employs two advanced constitutive models: (1) the *DamagePlasticityConcreteECT* model for concrete, based on a modified EN 1992-1-2 [3] formulation that explicitly accounts for transient creep, plastic deformation, and damage evolution; and (2) the *DPMsteelEC* model for steel reinforcement, implementing the EN 1992-1-2 [3] stress-strain relations to capture temperature-dependent plasticity and strength degradation in reinforcing steel.

2.2 GID-OpenSees interface and workflow

The developed framework is seamlessly integrated through the GiD-OpenSees interface, offering an automated workflow for simulating RC structures under both fire and PEF conditions. As illustrated in Fig. 1, the comprehensive platform handles all analysis phases: (1)

pre-processing (geometry creation, section discretization, and material assignment), (2) sequentially coupled thermo-mechanical analysis, and (3) post-processing. The interface enables users to define temperature-dependent material models for concrete and steel reinforcement. User can also choose different fire scenarios. The analysis proceeds through two key stages: first, heat transfer analysis which runs in OpenSees and stores temperature time histories for each fiber in a .dat file; subsequently, mechanical analysis is executed in OpenSees via an automatically generated .tcl script.

3 EXPERIMENTAL VALIDATION

The numerical framework is validated against two distinct experimental cases (Fig. 2, Table 1): (1) an undamaged column (C1) tested under natural fire condition [12], and (2) a seismically damaged column (C2) subjected to post-earthquake fire exposure [13]. The column C1 was designed as per ACI 318 specifications and subjected to axial loading of 403 kN, representing 55% of its factored design load capacity (732 kN). The column was exposed to fire which follows ASTM E119 heating for 120 min followed by a decay phase of $-5.5\,°$C/min at its four faces in the central region (Fig. 2a). The comparison of the predicted thermal and mechanical response against the experimental values are shown in Fig 3. The thermal response of column C1 shows a rapid temperature increase during the initial heating phase, followed by decrease in temperature in the later stage (cooling). During the heating phase, the temperature in the concrete and reinforcement rises, with surface temperatures reaching approximately $800\,°$C, while the inner core remains significantly cooler due to the low thermal conductivity of concrete. Whereas this trends reverses during the cooling phase of the fire. It should be noted that temperature peaked at the core (location 3) during the cooling phase at nearly 250 min. The mechanical response follows a typical thermo-mechanical pattern, with initial axial expansion due to thermal effects, reaching peak displacement before transitioning into contraction caused by material degradation and creep. The rate of contraction is much steeper than the recovery phase. Residual deformation remains after cooling due to irreversible damage in concrete and reinforcement. Overall the numerical results closely agrees the experimental trends.

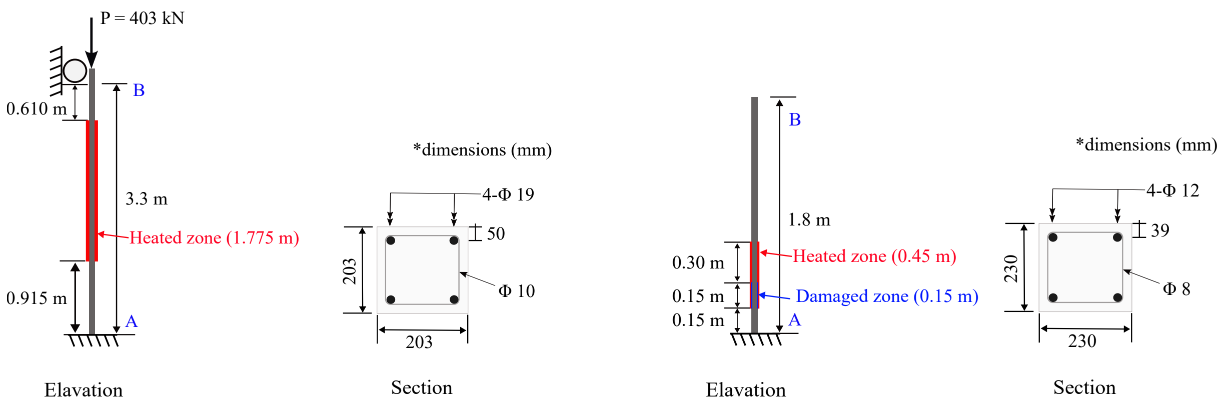

(a) Column 1. (b) Column 2.

Figure 2: Schematic of the columns considered for validation and numerical study.

The experimental protocol for Column C2 involved a sequential loading procedure to simulate post-earthquake fire conditions. First, the column was subjected to combined axial loading and reverse cyclic displacements to induce seismic damage, characterized by concrete spalling to 20 mm depth over a 0.15 m region near the column end (Fig. 2a). Following damage ini-

Column	C 1	C 2
Tested by	Kodur et al. [12]	Chinthapalli and Agarwal [13]
Concrete compressive strength, f_c	62 MPa	25.3 MPa
Rebar yield strength, f_y	420 MPa	500 MPa
Axial load	403 kN	—
Test fire scenario	ASTM E119 heating with linear decay phase	ISO 834

Table 1: Properties of the columns considered in validation study.

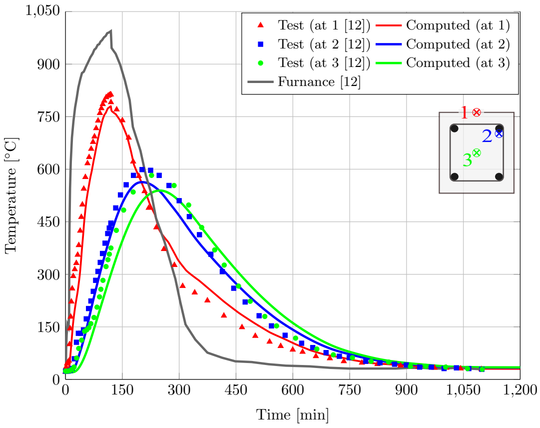

(a) Comparison of temperature inside mid-height section.

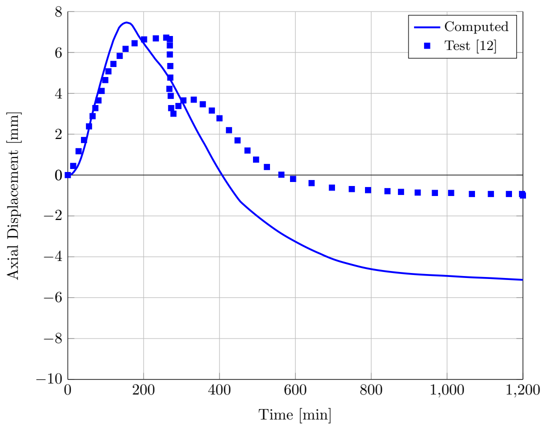

(b) Comparison of axial displacement of column top.

Figure 3: Comparison of predicted and measured value for column C1.

tiation, the mechanical loads were removed and the column was exposed to ISO 834 standard fire for 60 minutes along a 450 mm length encompassing the damaged zone (Fig. 2b). Finally, axial loading was reapplied until structural failure occurred. In the simulation the column was modelled using 24 beam elements and 23×23 fibers in the undamaged sections. The damaged section is modelled by removing the outer fiber upto the cover depth of 20 mm. The damaged-column is subjected to ISO 834 fire and then axial load is incrementally increased till failure. As shown in Fig. 4, the numerical load-displacement response demonstrates excellent agreement with experimental results, with less than 5% deviation in peak load capacity. The result demonstrate excellent predictive capability for simulating the PEF performance of RC columns.

4 NUMERICAL STUDY

This study investigates the post-earthquake fire performance of RC columns through the previously developed model. The previously validated model for undamaged column C1 was adapted to systematically assess the structural behavior under natural fire exposure with varying degrees of seismic damage. Three damage states are considered in this study: D0 (Immediate Occupancy level with an intact section or minor cracking), D1 (Life Safety level with 50% cover spalling), and D2 (severe damage with complete cover loss and exposed reinforcement). The damage is uniformly applied across all 4-faces of the column near the heated zone at a stretch of 300 mm. The heated zone of the column is extended to 2.7 meters along the central

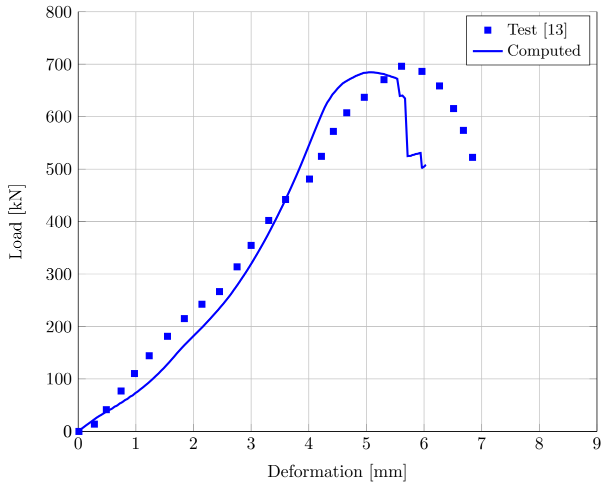

Figure 4: Comparison of predicted and measured load vs displacement for column C2.

region (Fig. 2a) to simulate realistic conditions. Three parametric natural fire scenarios – F-60, F-90, and F-120 – are developed following EN 1991-1-1 (Annex A) guidelines (Fig. 5) and are considered in the fire resistance evaluation of column under PEF scenarios.

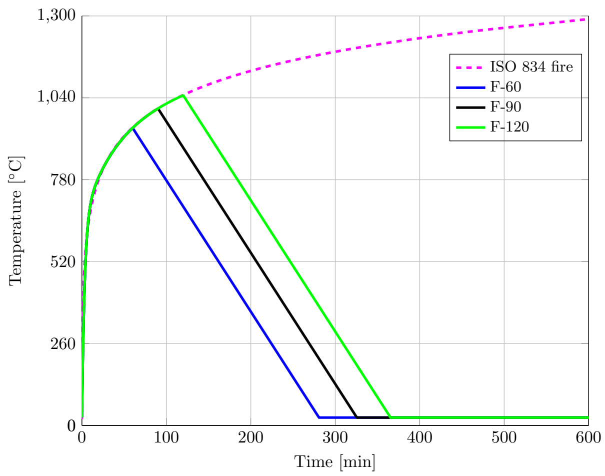

Figure 5: Different fire scenarios considered.

4.1 Influence of fire scenarios

This section examines the structural response of Column C1 with three damage states (D0-D2) under different fire scenarios (F-60, F-90, and F-120) with four side exposure. Figure 6 presents the axial displacement responses of the column under each fire scenario. For F-60 exposure, while columns with minor (D0) and moderate (D1) damage survived, the severely damaged column (D2) failed at 55 min during heating phase. This early failure suggests that extensive prior damage significantly reduces fire resistance. Notably, since the heating phase is identical across all fire scenarios until 60 minutes, D2 columns would fail at the same time (55 min) in F-90 and F-120 exposures, as indicated by the dashed line in Figure 6. Under F-90 exposure, the undamaged column (D0) maintained structural integrity till the end of the fire, while the column (D1) failed at 117 min during cooling. This cooling-phase failure highlights the critical influence of thermal inertia on damaged structures. In contrast, for the more severe F-120 scenario, both damaged states failed one during heating (D1 at 113 min) and one during cooling (D2 at 155 min). It should be noted that the column with damage D1 fails during the cooling in F-90 while it fails during heating in F-120. This is likely resulted due to the column reaching similar states in the two fire scenarios at the time of failure.

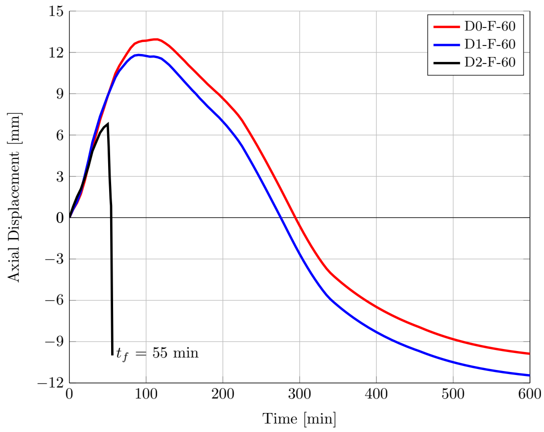

(a) Axial displacement response under F-60.

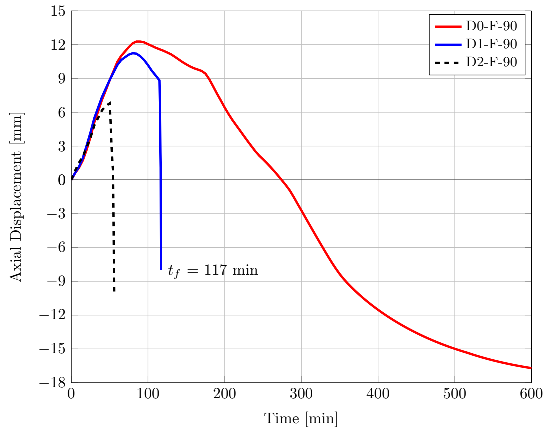

(b) Axial displacement response under F-90.

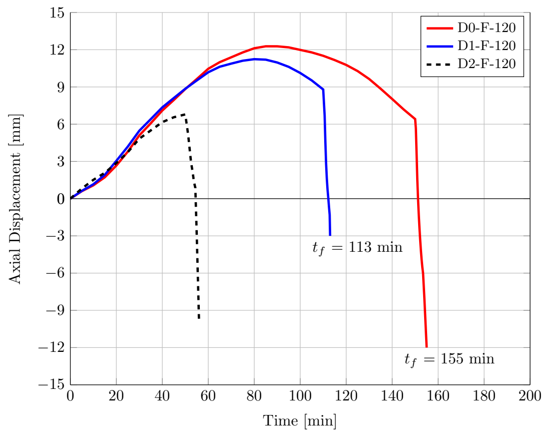

(c) Axial displacement response under F-120.

Figure 6: Column C1 with damage D0, D1 and D2 under various fire scenarios.

4.2 Influence of fire exposure configurations

This section examines the influence of fire exposure configurations (i.e., number of exposed faces) on the performance of RC columns with damage states D0-D2 under F-120 fire condition. The results (Table 2) demonstrate significant variations in structural response based on exposure configurations. For single-face exposure, all columns maintained structural integrity regardless of its damage state. The residual capacity of the column are also evaluated in this case by incrementing the axial load at the conclusion of fire until failure. The residual capacity shows minimal variation for damage state D0 and D1, while it reduces significantly in case of D2. The failure patterns under multi-face exposure showed distinct trends: undamaged columns

(D0) failed much later under three-face exposure (535 min, cooling phase) compared to four-face exposure (155 min). This demonstrates the protective effect of an unexposed face in case of undamaged column. However, damaged columns (D1 and D2) showed minimal variation ($< 5\%$) in failure times between three-face and four-face exposure. This behavior stems from thermal bridging through damaged regions and reduced sectional capacity.

Fire exposure side	Time (min) of failure under F-120		
	D0	D1	D2
One-sided	NO ($L = 758$ kN)	NO ($L = 753$ kN)	NO ($L = 638$ kN)
Three-sided	535	117	58
Four-sided	155	113	55

$\star$ L refers to residual load capacity of the column after cooling upto 600 min.

Table 2: Comparison of fire resistance time for various damage condition under one-side, three-side and four-side F-120 fire exposure.

4.3 Influence of load ratios

This section investigates the influence of load ratio (30%, 40%, 55% of the 732 kN design capacity) on the fire performance of columns with varying damage states (D0-D2) under different fire scenarios (F-120, F-90, F-60). The results (Fig. 7) demonstrate a clear relationship between load ratio and structural resilience: (1) For undamaged columns (D0), reducing the load ratio from 55% to 40% increased the failure time by 56% (from 155 to 242 minutes) under F-120 exposure, while the column survived entirely at 30% loading; (2) Moderately damaged columns (D1) withstood both 30% and 40% load ratios without failure; (3) Severely damaged columns (D2) showed improved but limited resistance, with failure delayed from 55 minutes (55% load) to 68 minutes (40% load) under F-60 exposure, while surviving at 30% loading. These findings as illustrated in Fig. 7, highlight that while load reduction enhances fire resistance across all damage states, the benefits are most pronounced for undamaged columns, with diminishing returns as damage severity increases. The results suggest that post-earthquake fire safety assessments should consider both residual capacity and reduced load ratios when evaluating structural performance.

5 CONCLUSIONS

A comprehensive investigation of the post-earthquake fire (PEF) performance of reinforced concrete (RC) columns was conducted using the GiD-OpenSees framework. The numerical framework was validated against two benchmark cases: one undamaged column and one column with predefined seismic damage. A detailed parametric study was then performed to assess the influence of key factors — namely, fire scenarios, fire exposure configurations, and axial load ratios — on the performance of damaged RC columns. Based on the findings, the following conclusions are drawn:

- Fire resistance significantly decreases with increasing seismic damage. Severely damaged columns (D2) fail early during the heating phase, regardless of fire duration.
- Columns may fail during the cooling phase, especially in longer fire durations (F-90, F-120), due to thermal inertia. This highlights the critical role of including the decay

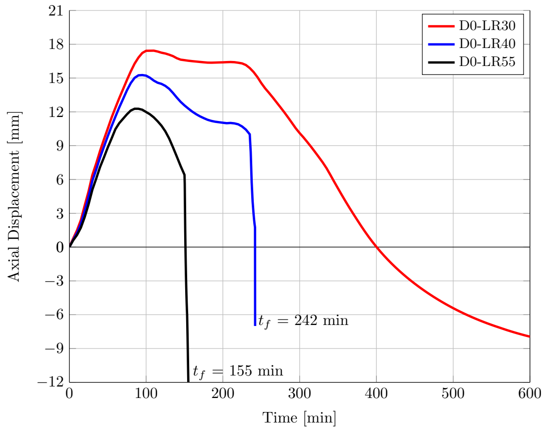

(a) Column with damage state D0 subjected to load ratio 30%, 40% and 55% under F-120.

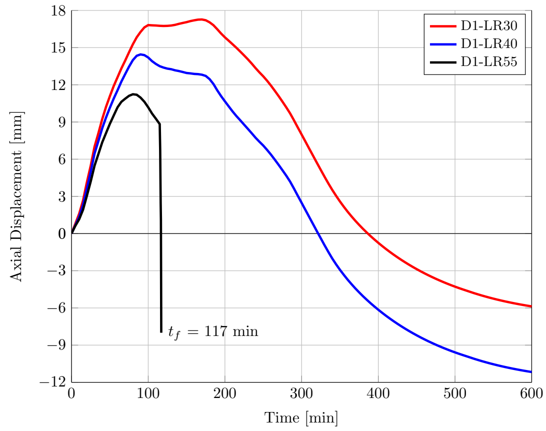

(b) Column with damage state D1 subjected to load ratio 30%, 40% and 55% under F-90.

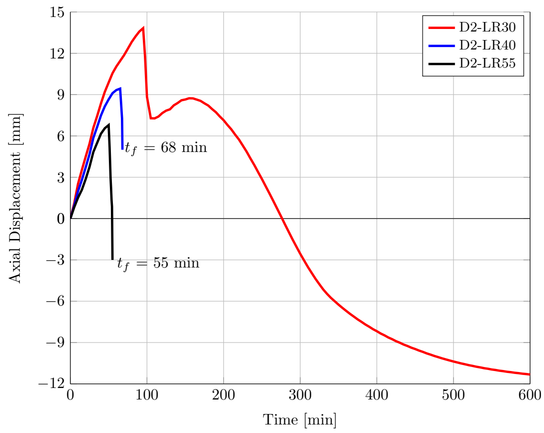

(c) Column with damage state D2 subjected to load ratio 30%, 40% and 55% under F-60.

Figure 7: Comparison of column with damage state D0, D1 and D2 subjected to different load ratios.

(cooling) phase in PEF analysis.

- More exposed faces lead to earlier failure. Undamaged columns benefit from partial protection (e.g., 3-face vs. 4-face exposure), but this benefit diminishes for damaged columns due to thermal bridging and reduced cross-sectional capacity.
- Lower axial load ratios improve fire resistance for all damage states. The enhancement is most significant for undamaged columns and reduces with increasing damage severity.

6 ACKNOWLEDGMENTS

The second author gratefully acknowledges the financial support of the DRDO armaments research board, India (ARMREB/STE/2022/265).

REFERENCES

[1] S. Mousavi, A. Bagchi, and V. Kodur, Review of post-earthquake fire hazard to building structures. *Canadian Journal of Civil Engineering*, **35(7)**, 689–698, 2008.

[2] NRCC 2005, *National building code of Canada 2005*. Canadian Commission on Building and Fire Codes, National Research Council of Canada, Ottawa, Ont.

[3] EN 1992-1-2, *Design of Concrete Structures—Part 1–2: General Rules—Structural Fire Design*. London: European Committee for Standardization, 2004.

[4] ACI 216.1-14, *Code Requirements for Determing Fire Resistance of Concrete and Masonry Construction Assemblies*. American Concrete Institute, 2014.

[5] T. Gernay et al., Experimental Investigation of Structural Failure during the Cooling Phase of a Fire: Concrete Columns. *Fire Safety Journal*, **134**, 445–460, 2022.

[6] U. Sharma et al., Testing of full-scale RC frame under simulated fire following earthquake. *Journal of Structural Fire Engineering*, **5(3)**, 215–228, 2014.

[7] B. Behnam and H. R. Ronagh, Performance of reinforced concrete structures subjected to fire following earthquake. *European Journal of Environmental and Civil Engineering*, **17(4)**, 270–292, 2013.

[8] B. Behnam and H. R. Ronagh, Post-earthquake fire resistance of CFRP strengthened reinforced concrete structures: using carbon fiber polymers to improve post-earthquake fire resistance. *The Structural Design of Tall and Special Buildings*, **23**, 814–832, 2014.

[9] H. Vitorino, H. Rodrigues, and C. Counto, Evaluation of post-earthquake fire capacity of a reinforced concrete one bay plane frame under ISO fire exposure, *Structures*, **23**, 602–611, 2020.

[10] H. Vitorino, H. Rodrigues, and C. Counto, Evaluation of post-earthquake fire capacity of reinforced concrete elements. *Soil Dynamics and Earthquake Engineering*, **128**, 105–900, 2020.

[11] A. Kumar, P. R. Prakash, and M. A. Orabi, Modeling reinforced concrete structures under fire conditions in GiD-OpenSees: Framework, validations, and implications. *Advances in Engineering Software*, **201**, 103–855, 2025.

[12] V. Kodur, D. Hibner, and A. Agrawal, Residual response of reinforced concrete columns exposed to design fires. *Procedia engineering*, **210**, 574–581, 2017.

[13] H. K. Chinthapalli and A. Agarwal, Fire performance of earthquake-damaged reinforced concrete columns: an experimental study. *Journal of structural fire engineering*, **13(1)**, 67–87, 2002.

[14] J. M. Franssen and T. Gernay, Modeling structures in fire with SAFIR®: Theoretical background and capabilities. *Journal of Structural Fire Engineering*, **8(3)**, 300–323, 2017.